Preparation, characterization, and *in vivo* evaluation of a fluconazole-loaded chitosan lipid nanoparticle hydrogel in a rat wound model infected with fluconazole-resistant *Candida albicans*

Rawia M. Khalil[1], Marwa A. Wagdi[1], Shaymaa A. Ismail[2], Amira A. Hassan[2], Marwa E. Shabana[3], Ahmed A. Sedik[4], and Eman S. Shalaby[1]*

ABSTRACT

Fungal infections are among the most serious dermatological disorders and affect more than 25% of the global population. *Candida albicans* infection is considered the most widespread fungal infection. This research aims to assess the effect of the topical application of fluconazole (FLU) lipid nanoparticles (LNPs) loaded in a chitosan natural biopolymer hydrogel (FLU–LNP–CHI) on a rat wound excision model infected with *C. albicans*. Four formulations (F1–F4) were chosen based on the encapsulation efficacy findings (ranging from 12.1% to 72.5%). Chitosan biopolymers were used to enhance the antimicrobial effect, viscosity, and industrial applicability of LNPs. The particle size (251.6–409.0 nm) and zeta-potential (22.82–51.73 mV) of the formulations were determined. In the *in vitro* antifungal study, F2 (zone of inhibition = 23 ± 0.4 mm) showed better antifungal properties than F4 (zone of inhibition = 21 ± 0.7 mm). After several assessments, F2 and F4 were selected for evaluation of their biological effectiveness in healing *C. albicans*-infected wounds. Histological and *in vitro* antifungal analyses were used to evaluate the subsequent healing process. The results confirmed that FLU–LMP–CHI can accelerate wound healing by increasing indices of skin regeneration, as evidenced by histopathological studies. Our findings indicate that, compared with FLU alone, FLU–LNP–CHI has significant potential to improve the healing of FLU-resistant *C. albicans*-infected wounds due to its potent antifungal properties.

Keywords:
Fungal infection; *Candida albicans*; Wound; Chitosan; Fluconazole; Histopathology

***Corresponding author:**
Eman S. Shalaby,
Dremanshalaby_nrc@hotmail.com

How to cite this article:
Khalil RM, Wagdi MA, Ismail SA, *et al.* Preparation, characterization, and *in vivo* evaluation of a fluconazole-loaded chitosan lipid nanoparticle hydrogel in a rat wound model infected with fluconazole-resistant *Candida albicans*. *Biomater Transl.* 2026, 7(3), 425-434.

doi: 10.12336/bmt.25.00026

1. Introduction

The prevalence of severe wound infections and chronic wounds has increased rapidly in recent years. Open wound spaces offer a suitable, moist, and nourishing environment, but they can also be colonized by bacteria, and persistent infection may cause skin loss.[1] A wound infection may evolve from colonization without impairing healing to systemic infection with organ failure and sepsis. Risk factors for wound infection include smoking, diabetes, obesity, malnutrition, and patient age. Chronic skin wounds and infections, recognized as leading causes of morbidity and mortality, are thought to affect 1–2% of people in underdeveloped nations.[2] *Candida albicans* is a commensal microorganism commonly found on the skin and mucous membranes and has pathogenic potential under certain conditions, such as a compromised immune system, a high risk of invasive candidiasis, and increased resistance to available antifungal drugs.[3]

To accelerate the healing cascade, the components of the wound-healing formula are essential. For the majority of *C. albicans*-induced infections in both immunocompromised and immunocompetent individuals, fluconazole (FLU), a bisazole antifungal, is the primary treatment option (typically 100 mg/day for

1–2 weeks).[3] Like other triazoles, FLU prevents the production of ergosterol in fungal cell walls.[3,4] When FLU is taken orally, the gastrointestinal tract is disturbed (bloating, vomiting, and stomach pain), leading to irritation and severe hepatotoxicity.[4] Alternative topical methods should be preferred for treating candidiasis to minimize side effects and medication resistance while offering localized delivery. However, solubilizing FLU in lipid nanoparticles (LNPs) could increase its skin availability because its hydrophobic nature can pose challenges for topical formulations.[5]

Interest in drug delivery is growing as various nanocolloidal delivery methods are used to increase the bioavailability of medications. LNPs are advantageous as topical delivery systems due to their nanoscale size and appropriate surface functionalization. However, a significant limitation of LNPs is their low viscosity, which impairs their ability to adhere to the skin.[6] By adding an appropriate gelling agent, such as chitosan (CHI), LNPs can be transformed into high-viscosity delivery agents, resolving the low-viscosity issue[7] and enhancing stability and skin retention for a long time.[6] CHI, an N-deacetylated derivative of chitin, is a polycationic polymer primarily composed of glucosamine units. According to studies, CHI has anti-inflammatory and antioxidant properties, as well as other desirable biopharmaceutical qualities, such as antibacterial activity, biocompatibility, biodegradability, and bioadhesion.[8,9] This polycationic polymer has demonstrated promise as a drug carrier by forming a core–shell nanostructure through interactions with negatively charged molecules.[8] The interaction between the two components increases the residence time of the formulation on the skin, thereby facilitating drug diffusion.

This research aims to develop and investigate a topical FLU-loaded LNP CHI gel (FLU–LNP–CHI) for the management and healing of *C. albicans*-infected skin wounds. Searches were conducted using Google Scholar and Google.com to identify relevant studies. Studies were selected based on the following criteria: inclusion criteria encompassed rats with standardized excisional wounds infected with FLU-resistant *C. albicans*, while exclusion criteria ruled out animals with systemic illness or contaminated wounds. Formulations were considered if they demonstrated low particle size, high zeta potential (ZP), high drug encapsulation efficiency (EE), and an optimum hydrogel pH. Evaluation criteria focused on wound healing, with successful formulations confirmed by restoration of normal skin structure in treated rats.

2. Materials and methods

FLU was a gift from Tenth of Ramadan for Pharmaceutical Industries and Diagnostic Reagents (Rameda), Egypt. Non-hydrogenated soybean phosphatidylcholine lipoid S100 and Lipoid SPC-3 were purchased from Lipoid GmbH, Germany. Soy lecithin was purchased from AVI-Chem Laboratories, India. Egg yolk lecithin (PL-30S) was a kind gift from Kewpie, Japan. Isopropyl myristate and 2,2-diphenyl-1-picrylhydrazyl (DPPH) were procured from Sigma Chemical Company (United States). CHI (degree of deacetylation >90%, average molecular weight = 250,000 g/mol, viscosity = 30–100 cP) was purchased from Glentham Life Sciences (United Kingdom [UK]). All other solvents and chemicals were of analytical grade and suitable for use in laboratory settings. A total of 40 Wistar rats were used in this study.

2.1. Preparation of FLU-loaded LNP-based chitosan hydrogel

The FLU–LNP–CHI was prepared via high-pressure homogenization and ultrasonication, with minor modifications to the standard procedure.[6] In brief, FLU was added after the designated lipids—Tween 80 and isopropyl myristate—were heated to 5°C above the melting point, and the heated mixture was then swirled onto a hot magnetic plate. The resulting primary emulsion was homogenized after ultrasonic agitation for 3–5 min. To create LNPs, they were then chilled in an ice bath at 4°C. In the second phase, FLU–LNPs were incorporated into the hydrogel, employing CHI as the gelling agent. A solution of CHI (1.0% w/v) was prepared on a hot magnetic plate by allowing it to swell in 0.1% acetic acid. The resulting LNP formulation was then gradually poured into the CHI solution while being stirred continuously throughout the addition. To ensure a clear and uniform preparation, the resulting mixture was swirled for an additional 30 min after combining. **Table 1** lists the components of FLU–LNP–CHI formulations.

2.2. EE

The entrapment of FLU-LNPS-CHI was determined via an indirect method. The prepared formulations were centrifuged (Union 32R, Hanil, Korea) at 7,000 rpm at –4°C for 40 min, and the quantity of unentrapped medications in the nanoparticles in the supernatant was calculated. A UV-visible (UV-Vis) spectrophotometer (2401/PC, Shimadzu, Japan) was used to determine the amount of unentrapped medicines at 261 nm.[10] The EE of FLU was determined through the following equation:[11,12]

$$\mathrm{EE}(\%) = \frac{\text{Total amount of drug} - \text{Amount of free drug}}{\text{Total amount of drug}} \times 100\% \quad (1)$$

Formulations that showed the greatest encapsulation potential were selected for further studies.

2.3. Particle size, polydispersity index, and ZP

Distilled water (10 mL) was added to a small amount of FLU–LNP–CHI, and then the mixture was shaken for 5 min,

[1]Department of Pharmaceutical Technology, Pharmaceutical and Drug Industries Research Institute, National Research Centre, Dokki, Giza, Egypt; [2]Department of Chemistry of Natural and Microbial Products, Pharmaceutical and Drug Industries Research Institute, National Research Centre, Dokki, Giza, Egypt; [3]Department of Pathology, Medical Research and Clinical Studies Institute, National Research Centre, Dokki, Giza, Egypt; [4]Department of Pharmacology, Medical Research And Clinical Studies Institute, National Research Centre, Dokki, Giza, Egypt

Table 1. Composition and encapsulation efficiencies of the prepared FLU–LNP

Formulation	Lipid type	Oil: Lipid ratio	Tween 80 (%)	Chitosan (%)	EE (%)
F1	SP3	5:1	1	1	43.86±1.04
F2[a]	LS100	5:1	1	1	72.35±1.05
F3	Soy lecithin	5:1	1	1	26.47±3.12
F4[a]	Egg lecithin	5:1	1	1	72.01±1.67
F5	SP3	3:1	1	1	37.67±0.21
F6[a]	LS100	3:1	1	1	67,72±0.84
F7	Soy lecithin	3:1	1	1	24.55±1.25
F8[a]	Egg lecithin	3:1	1	1	67.14±0.21
F9	SP3	2:1	1	1	25.14±0.42
F10	LS100	2:1	1	1	31.48±0.21
F11	Soy lecithin	2:1	1	1	12.10±0.22
F12	Egg lecithin	2:1	1	1	43.56±0.24

Note: [a]Selected for further investigation.
Abbreviations: EE: Encapsulation efficiency; FLU: Fluconazole; LNP: Lipid nanoparticle.

followed by short-term bath sonication. After that, the sample was placed in a quartz cuvette for photon correlation spectroscopy analysis at room temperature using a Malvern Zetasizer Nano ZS (Malvern Instruments, UK) to estimate particle size, polydispersity index (PDI), and ZP.[6,12,13]

2.4. *In vitro* FLU release efficiency

In vitro FLU release was investigated via the dialysis bag method.[14] The study was conducted with 10% ethanolic phosphate buffer (pH 5.5).[15,16] A quantity of each selected nanoformulation equivalent to 1 mg FLU was placed in each dialysis bag (cut-off molecular weight = 14 kDa) and sealed. The amber-colored glass bottles, holding the sealed dialysis bags, contained 100 mL of ethanolic phosphate buffer and were maintained at 32 ± 0.5°C[17] and 100 rpm for 24 h.[16,18] At 1, 2, 3, 4, 6, and 24 h, a 2 mL sample was obtained, and an equivalent volume of medium was added. The FLU regression equation in ethanolic buffer was used to assess the samples spectrophotometrically at 261 nm. Next, the FLU release efficiency (RE) was calculated. The results were analyzed kinetically using release models, such as zero-order, first-order, and Higuchi models, to assess the release mechanisms. Based on the release data, two formulations were selected for further testing.

2.5. Transmission electron microscopy (TEM)

The morphology of the selected formulations was investigated to assess their structural characteristics, particularly size and shape uniformity. FLU–LNP–CHI formulations were diluted with distilled water (1:10). One drop of the dilution was applied to a 300-mesh carbon-coated grid and left to air-dry at room temperature. Before the film had completely dried, it was adversely stained with 1% phosphotungstic acid. Micrographs were taken at appropriate magnifications through TEM (JEM-1230, JEOL, Japan) at room temperature and an acceleration voltage of 80 kV.

2.6. Rheological characteristics

A parallel-plate rheometer (Physica MCR 301, Anton Paar, Germany) was used to measure the rheological characteristics of FLU–LNP–CHI at 25 ± 0.5°C.[18] The rheometer plate was filled with a 0.5 g sample, and the shear rate was gradually increased from 10 to 100 s^{-1}. Next, a ratio of 100–10 was used.[19] The viscosity maximum value and shear rate dependence were recorded. To examine the rheological characteristics of the formulations under study, viscosity curves (viscosity vs. shear rate) were plotted. The average of the duplicates was used to generate the plot. All rheological measurements were performed in duplicate ($n = 2$), and the average of the duplicate runs was considered as the measured value as reported by previous literature. In the current research, rheological characteristics are conducted in duplicate rather than triplicate due to some practical constraints, such as time consumption, cost, and the high reproducibility of modern rheometers.

2.7. Differential scanning calorimetry

A differential scanning calorimeter (DSC; DSC-60, Shimadzu Corporation, Kyoto) was used to perform a thermal analysis on FLU, LS100, CHI, and freeze-dried FLU–LNP–CHI. The samples were heated from 25 to 200°C, then cooled at 10°C/min. All thermograms were recorded and investigated for any inconsistencies, such as noticeable variations or new peak appearances.[20,21]

2.8. pH measurement

The pH of the hydrogels was determined at ambient temperature with a pH meter (Jenway, Bibby Scientific Limited, UK) after calibration with buffer solutions (pH 7.0 and 10.0). The pH was measured after 0.5 g of FLU–LNP–CHI was well mixed and diluted 10 times with distilled water. Three replicates were performed, and the mean ± standard deviation is shown.

2.9. *Ex vivo* rat skin permeation

Modified Franz diffusion (FD) cells, with an effective diffusion area of 0.77 cm^2 and a receiver chamber capacity of 50 mL, were used for this investigation. A permeation experiment was conducted using rat skin. The rat's belly hair was shaved using a razor. Before use, the rat skin pieces were soaked in the media for 45 min. Next, 10% ethanolic phosphate buffer (pH 7.4) was added to the receiving compartments.[14] Water circulation was maintained at 37°C,[13] while the fluid in the receiving chamber was constantly rotated by a magnetic stirrer. Each donor compartment was filled with 1 g of evenly distributed selected FLU–NLP–CHI, which was then sealed to create an occlusive environment. To maintain sink conditions, a 2 mL sample was removed at 1, 2, 3, 4, 6, and 24 h, and an equivalent volume of medium was added. The total quantity of the medication that permeated the samples was calculated at 261 nm via a UV-Vis spectrophotometer.

2.10. Skin deposition study

After the permeation experiment, the skin placed on the FD cells was removed and washed three times with phosphate buffer. After adding 10 mL of methanol, the mixture was subjected to 1 h of bath sonication. After being chopped, the skin samples were incubated for 24 h in a refrigerator at 4°C with 10 mL of methanol. Each sample was thereafter filtered via a 0.2 µm syringe filter. The amount of FLU present in the skin layers was calculated spectrophotometrically at 261 nm.[13,22]

2.11. Irritancy test

To evaluate the skin-irritation potential of the medication and the optimized hydrogels, a skin-irritation experiment was conducted on Wistar rats. For the study, nine healthy rats were given unrestricted access to food and drink. To prevent peripheral injury, the backs of the rats were carefully shaved 24 h before the study. Each rat's left side of hairless skin received a uniform application of approximately 0.05 mL of formulation, whereas the right side served as a control. At 24, 48, and 72 h following application, the dorsal skin surface (left side) was checked for any obvious changes, such as erythema (redness). The degree of erythema was recorded according to the erythema score, with the following definitions: No erythema = 0, slight erythema (barely visible light pink) = 1, moderate erythema (dark pink) = 2, moderate-to-severe erythema (light red) = 3, and severe erythema (extreme redness) = 4.[17]

2.12. *In vitro* antifungal activity

In the present study, an FLU-resistant strain of *C. albicans* (ATCC 10231) was used to examine the antifungal activity of the prepared FLU–LNP–CHI formulations via the well-diffusion method.[23] The initial step involved uniformly spreading 200 µL of pre-cultured Sabouraud dextrose broth (equivalent to a 1 McFarland standard solution) on agar plates of the same medium. The wells (diameter = 7 mm) were subsequently produced in each agar plate via a sterile glass Pasteur pipette. A total of 100 µL of dimethyl sulfoxide (DMSO) solution of the tested formulations (containing 2.5 mg drug/mL) was added to separate wells, with DMSO alone serving as a control. The inhibition zone was measured in mm after incubation for 1 day at 30°C. Moreover, the minimal inhibitory concentration (MIC; the lowest concentration of the prepared formulation that inhibited *Candida* growth) was determined using different concentrations of the prepared formulations.

2.13. *In vitro* antioxidant activity

The Brand–Williams method was used to determine the antioxidant activity, which depends on the scavenging of DPPH free radicals.[24] A stock methanolic solution of DPPH was initially prepared (24 mg of DPPH dissolved in 100 mL of methanol). Thereafter, 3.9 mL of the diluted solution (10 mL of the stock solution diluted with 45 mL of methanol) was added to 0.1 g of the prepared formula, which was shaken well and then left to stand for 24 h in the dark. Any reduction in absorbance was assessed at 515 nm, and the antioxidant potential was expressed as µM of Trolox equivalents (TE) per gram of formulation sample.

2.14. *In vivo* study

The rats were placed under general anesthesia, after which an incision (1.5 × 1.5 cm) was made between their shoulders. After that, 0.1 mL of a solution containing 1.5×10^7 colony-forming units of *C. albicans* yeast was administered to the wound, leading to infection within 24 h. The animals (except those for the healthy control) were randomly distributed into four groups: Group 1 was the unwounded healthy control; Group 2 was the untreated, infected negative control; and Group 3 received the blank formulation, whereas Groups 4 and 5 received free-FLU suspension and the FLU–LNP–CHI (F2) hydrogel, respectively (8 animals/group). The FLU–LNP–CHI hydrogel was administered before the start of wounding. The formulations were topically administered to the wound area once daily, beginning 24 h after the first operation and lasting for 20 days. Every rat was inspected for infection or any fluid in the wounds.[25]

2.15. Histopathology

We collected rat tissues from each group. The samples were dehydrated, washed in xylene, and embedded in paraffin blocks after fixation for 48 h in 10% buffered formalin solution. Serial 5 µm sections were mounted, washed in a water bath, and dewaxed in an oven using glass slides. The slices were stained with hematoxylin and eosin. Histopathological changes were assessed using an Olympus CX41 light microscope (Japan). We processed the photomicrographs via Adobe Photoshop version 8.0.

2.16. Statistical analysis

Statistical analysis was performed using Statistical Package for the Social Sciences (version 28.0, IBM, United States). Data are expressed as mean ± standard deviation. Differences among multiple groups were evaluated using one-way analysis of variance (ANOVA). When a statistically significant difference was detected, Fisher's Least Significant Difference (LSD) and Tukey's Honestly Significant Difference (HSD) *post hoc* tests were applied to identify intergroup differences. A value of $p<0.05$ was considered statistically significant.

3. Results and discussion

3.1. EE

The EE of the prepared formulations is listed in **Table 1**. A high EE and amount of drug in the matrix reduced the amount of drug used. The average EE values were in the following order: nanoparticles containing egg lecithin (hydrophilic–lipophilic balance [HLB] = 7)[26] > nanoparticles containing LS100 (HLB = 8.6)[27] > nanoparticles containing SP3 (HLB = 8.3) > nanoparticles containing soy lecithin (HLB = 9.2).[28] The EE of egg lecithin was very high because it has the lowest HLB, resulting in good solubilization of FLU in the hydrophobic region of the lipid particles. An increase in the HLB decreases the EE of lipophilic drugs,[29] as the solubility of FLU in the hydrophobic phase of the nanoparticles decreases, allowing FLU to be easily diffused from the lipid matrix. Increasing the lipid concentration clearly led to a noticeable reduction in EE. This could be due to the repulsion between the negative charges on the drug[30] and the negative charges on the lipids,[11] which facilitates expulsion of the drug from the nanosystems. Similar results have been reported for a decrease in EE after the inclusion of a negatively charged component in nanosystems.[31] F2, F4, F6, and F8, which showed the highest EE, were selected for further investigations.

3.2. Particle size and ZP

The particle size, ZP, and PDI values are displayed in **Table 2.** The particle size ranged between 251.6 and 409.0 nm. Particle

Table 2. Particle size (PS), zeta potential (ZP), polydispersity index (PDI), and release efficiency (RE) of the selected formulations

Parameter	F2	F4	F6	F8	Free FLU
Drug released (%)					
0 h	0	0	0	0	0
1 h	19.54±0.04	22.98±1.17	23.37±1.64	20.03±1.02	12.87±0.37
2 h	25.93±1.28	29.83±2.52	31.11±2.45	37.90±3.18	20.35±1.32
3 h	30.22±3.77	33.33±2.47	37.08±0.92	45.38±0.21	21.52±0.58
4 h	32.47±2.47	33.79±0.95	38.18±1.56	47.78±0.63	22.22±1.54
6 h	32.85±0.98	34.42±0.34	39.14±3.15	51.12±0.42	22.77±0.34
24 h	41.14±1.25	44.02±1.21	53.27±2.47	73.71±0.61	26.79±1.85
RE_{0-24} (%)	34.29±0.64	36.55±3.54	42.45±3.87	56.22±0.33	23.20±2.23
PS (nm)	409.00±0.22	251.60±2.29	304.90±1.25	255.50±2.35	-
ZP (mV)	32.71±1.44	22.82±0.97	51.73±2.67	30.39±2.93	-
PDI	0.442±0.09	0.441±0.02	0.405±0.03	0.425±0.05	-

Abbreviation: FLU: Fluconazole.

sizes less than 500 nm are reportedly appropriate for topical delivery.[32] An increasing oil: lipid ratio significantly decreased the particle size ($p<0.05$). A high oil content might lead to a decrease in viscosity, resulting in lower particle size values.[13] These observations are consistent with earlier reports.[33,34] The formulations selected for the current investigation showed promising EE, as mentioned in the previous section. Increased surface curvature and additional particles that engage in active interactions with molecules at the interface (such as surfactants) are the result of particles in the nanoscale range. The capacity of lipid molecules to form an ideal crystal decreases as surface curvature increases. This highlights the formation of amorphous systems that are capable of encapsulating FLU better.[35] The reasonable positive ZP values could be due to the presence of positively charged CHI on the surface of the nanoparticles, which might have contributed to the favorable stability of the FLU–LNP–CHI hydrogel.[36,37] Due to electrostatic repulsion, charged nanoparticles typically remain scattered in a stable manner.[38] All PDI values were less than 0.5, indicating the narrow size distribution of all the nanoparticles.[39]

3.3. *In vitro* drug release

The prepared FLU-LNP-CHI initially exhibited rapid release within 6 h, followed by sustained release over the subsequent 24 h (**Table 2**). The percentage release values ranged between 41.14% and 73.70% after 24 h. A rapid release of FLU was observed for 6 h in the first phase. The diffusion of untrapped adsorbed FLU onto formulation surfaces and the simple diffusion of the media into the system, followed by gradual release, could be the cause. The development of a thick gel matrix structure of CHI could be a cause of the delayed release[11] and subsequent immobilization, independent of the slow FLU release. Sustained release of FLU eventually enhances its bioavailability, thereby reducing the dosage and frequency of treatment.[6] The incorporation of CHI improved encapsulation and facilitated the formation of a diffusion barrier, thereby facilitating the controlled release of FLU from the prepared systems. The outcomes are in line with those of other previous investigations.[40] Changes in the oil: lipid ratio affect the rate of drug release from formulations. A decrease in the oil: lipid ratio from 5:1 to 3:1 increased drug release. This can be explained by the smaller particle size of the formulations with lower ratios, which allows easier diffusion of the drug from the prepared systems, as a higher surface area: Volume ratio facilitates the release and permeation of the entrapped drug through physiological drug barriers.[41] The reduced release of FLU from the suspension may be caused by the greater particle size or less porous structure (RE = 23.20%). Loading FLU into FLU–NLP–CHI increased its release from the semipermeable membrane (RE = 34.29% to 56.22%) due to the improved solubility and reduced particle size.[42,43]

Several mathematical models were used to analyze *in vitro* release profiles. The highest correlation coefficient (R^2) (data not shown) was obtained when the drug was released from all formulations and from its free suspension, as predicted by the Higuchi equation. As a result, FLU needs to dissolve in a lipid matrix, migrate to the matrix surface, and then separate into the polymer (CHI) layer. The FLU was then discharged into the surrounding medium. Similar results were reported by other authors.[44,45] F2 and F4, which have a reasonable release pattern, ZP, and particle size, were therefore selected for further studies.

3.4. TEM

TEM was performed to examine the morphological structure of F2 and F4 (**Figure 1**). The particles were spherical, with no aggregations. The extremely homogeneous morphology of the nanodroplets, along with the porous surface and tiny dark dots, demonstrated successful drug encapsulation in the prepared systems and a consistent particle size distribution. The particle size in the transmission photos is consistent with the Zetasizer results.

3.5. Rheological characteristics

The viscosity curves (viscosity vs. shear rate) of the selected formulations (F2 and F4) are displayed in **Figure 2.** A continuous reduction in viscosity was observed with increasing shear rate, indicating that the FLU–LNP–CHI systems exhibited pseudoplastic, non-Newtonian flow behavior. The viscosity of the

formulations fluctuated with changes in shear rate. The dependent change in viscosity is advantageous, as it facilitates the elimination of the formulation from the container and its application and spread over the skin. The network structure of the preparation disintegrates under shear force, leading to a progressive decrease in viscosity. F2 had higher viscosity values than F4 did, attributable to the semisolid nature of the phospholipid LS100[46] compared with the liquid nature of egg lecithin[47] at ambient temperature.

3.6. Differential scanning calorimetry

The thermograms of F2, F4, and individual components are shown in **Figure 3.** The DSC curve of pure FLU showed an endothermic melting peak (max. 138.4°C), indicating its crystalline state. This endothermic peak vanished in every formulation that was examined, suggesting that the produced formulations changed the crystalline form of FLU to the amorphous form. The complete solubilization of FLU in the system matrix could be the cause. The melting transition of CHI is shown by a wide endothermic peak in its DSC curve at approximately 100°C. This melting peak vanished after incorporation into the investigated formulations. This could be attributed to the large surface area of the nanometric particles and to the components of the investigated formulations. Similar results were previously reported.[18]

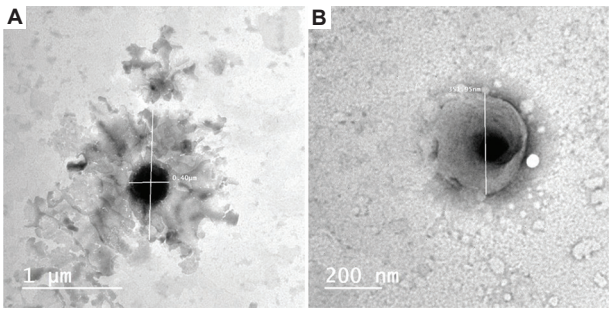

Figure 1. Transmission electron microscopy images of (A) F2 (scale bar: 1 µm; magnification: ×50) and (B) F4 (scale bar: 200 nm; magnification: ×50).

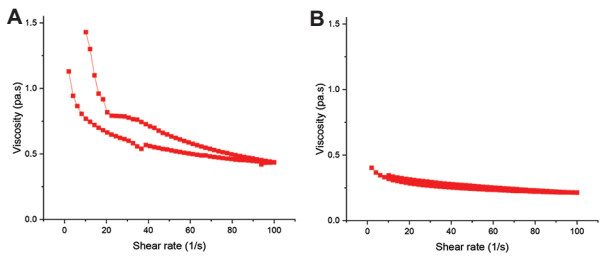

Figure 2. Rheological behavior of (A) F2 (n = 2) and (B) F4 (n = 2).

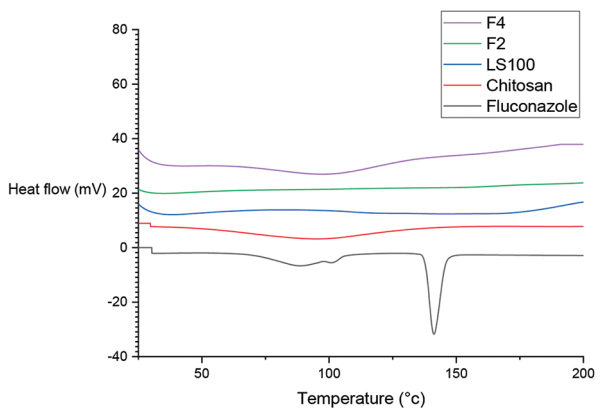

Figure 3. Differential scanning colorimetry curves of fluconazole, LS100, chitosan, F2, and F4 (all n = 2).

3.7. pH measurements

The F2 and F4 hydrogels had pH values of 5.97 ± 0.019 and 6.18 ± 0.038, respectively. The pH of the skin is between 5.0 and 7.0; thus, these numbers are appropriate.[17] Therefore, both hydrogels can be applied safely.

3.8. Permeation and skin deposition

Figure 4 presents the permeation profiles of FLU from its suspension and the chosen formulations (F2 & F4). Because lipid systems may encapsulate medications, maintain their release, extend the time that payloads remain in the skin, and effectively penetrate the skin barrier, they show considerable promise for the topical delivery of therapeutic substances.[37] Compared with the free FLU suspension, the FLU–LNP–CH systems presented higher permeation values. This can be attributed to the permeation-enhancing effects of CHI, lecithin, and phospholipids.[48-50]

F2 demonstrated lower permeation and higher skin deposition compared with F4, attributable to its higher viscosity, which hindered the penetration of FLU through the skin, thereby allowing greater deposition.

The formulations under investigation were able to deliver drugs to the skin layers appropriately. To effectively treat burn wounds, the findings show that the current preparation was efficient at depositing FLU into the skin layers and that the highest FLU concentration was present at the target locations (epidermis and dermis). Increased corneocyte interaction and skin blockage of CHI systems have been proposed as explanations for this dermal retention of FLU. Due to their tiny size, nanoparticles are more prone to interact with the superficial connections of cornocyte clusters and the furrows between cornocyte islands, thereby promoting their accumulation for an extended period. Consequently, it is postulated that highly lipophilic drugs encapsulated in nanoparticles form a "depot" within the stratum corneum, enabling their sustained release into deeper skin layers.[13]

3.9. Irritancy study

After topical treatment is applied to the skin, it can occasionally cause allergic reactions or irritation, including redness, edema, or scaling. To ensure the safety and viability of the formulations, careful evaluation of the effects of the ingredients in the topical formulation is needed. There were no apparent signs of skin irritation, erythema, or edema in the rat skin 24, 48, or 72 h after the administration of F2 or F4, according to visual grading (erythema score = 0).

3.10. *In vitro* antifungal activity

The *in vitro* antifungal potency of F2 and F4 was evaluated using FLU-resistant *C. albicans*. The results shown in **Table 3** indicate

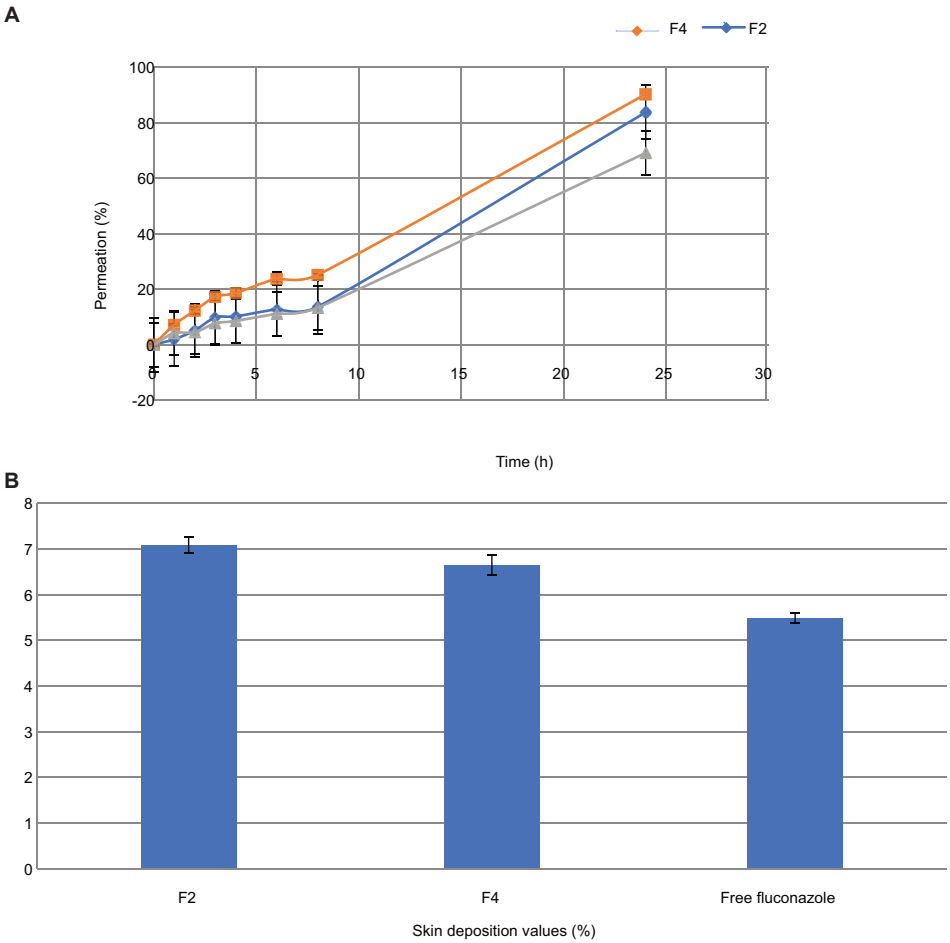

Figure 4. *Ex vivo* (A) skin permeation profiles and (B) skin deposition values of free fruconazole, F2, and F4 (all $n = 3$)

that both formulations exhibited antifungal activity against the examined strain, with F2 (MIC = 78 µg/mL) exhibiting a larger inhibition zone than F4. In the pharmaceutical field, the particle size of drugs is one of the most crucial criteria affecting their bioactivity and characteristics, such as saturation solubility and adhesiveness to membranes or surfaces, and various nanoparticles exhibit enhanced antifungal activity.[51] El Rabey *et al.*[52] reported that the loading of FLU in CHI nanoparticles strongly increased its biocidal activity against drug-resistant strains of *C. albicans*. In the present study, FLU alone did not result in any area of inhibition, possibly because the strain used in the experiment was resistant to the drug. Loading FLU into the formulation enhanced its effect on the resistant strain, resulting in a zone of inhibition. The larger inhibition zone of F2 was attributed to its constituents, as the blank F2 had an inhibition zone greater than that of the blank F4.

3.11. *In vitro* antioxidant activity

The use of antioxidants is pivotal for improving wound healing.[53] The DPPH scavenging potential of the investigated formulations was evaluated. The results indicate that F2 exhibited an activity of 2,773 ± 82 µM TE/g, which was much greater than the 1,554 ± 67 µM TE/g of F4. On the other hand, an equivalent amount of free FLU did not result in any antioxidant activity. This result might be due to the antioxidant activity of the formulation constituents (CHI, soybean phosphatidylcholine, and egg yolk lecithin).[54-56] Ultimately, F2 was selected for further investigation in *in vivo* experiments.

3.12. Histopathological examination

Histopathological examination of skin samples from different groups was performed to evaluate the effectiveness of the formulations, and micrographs are shown in **Figures 5** and **6**. Micrographs from the healthy control group (Group 1) revealed normal epidermal and dermal layers (**Figure 5A**). The skin from the negative control group (Group 2) exhibited inflammatory cell infiltration at the stratum corneum and upper epidermal layer (black arrow); neutrophilic aggregation at the skin surface with keratinization (green arrow); epithelial hyperplasia, acantosis, and moderate spongiosis formation (red arrow); and the presence of an edematous space between the dermal and epidermal layers (star) (**Figure 5B–F**).

Figure 6 shows micrographs of the treated groups (Groups 3–5) in comparison with Group 2. The tissue sections from Group 2 presented marked inflammatory cell infiltration and spongiosis (**Figure 5B**). Compared with Group 2, the group treated with the blank formulation (Group 3) did not significantly differ, as inflammatory cell infiltrates were still present in the superficial epidermal layer, and non-cellular keratin scale and hyperkeratosis were also observed (**Figure 6B**). The tissue sections from the free-FLU group (Group 4) presented mild

Table 3. Zone of inhibition of the selected formulations

Sample	Zone of inhibition (mm)
F2 (blank)	19±0.0
F2	23±0.4
F4 (blank)	17±0.0
F4	21±0.7
Fluconazole	-

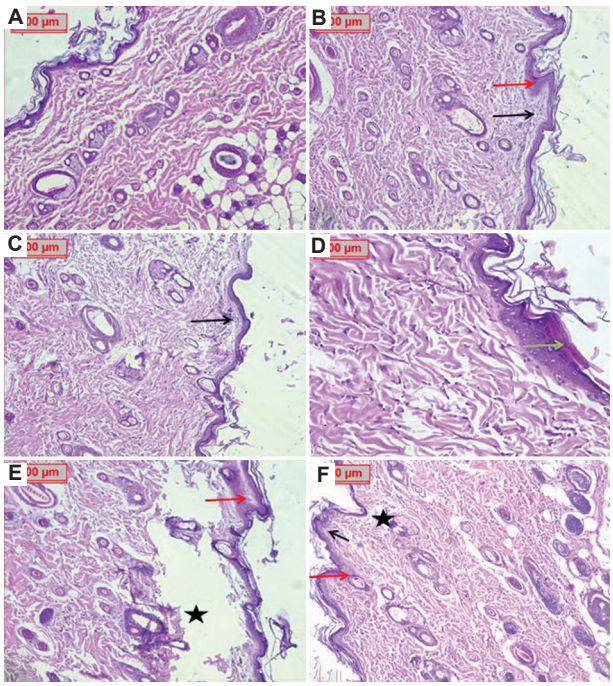

Figure 5. Hematoxylin and eosin staining showing histopathological changes in the skin of (A) healthy control (Group 1), demonstrating normal dermal and epidermal skin; and (B–F) untreated negative control (Group 2). Scale bars: (A–C, E, F) 200 μm, (D) 100 μm; magnifications: (A–F) ×50. Notes: Black arrow: Inflammation; Red arrow: Spongiosis formation; Green arrow: Keratinization; Star: Edematous space.

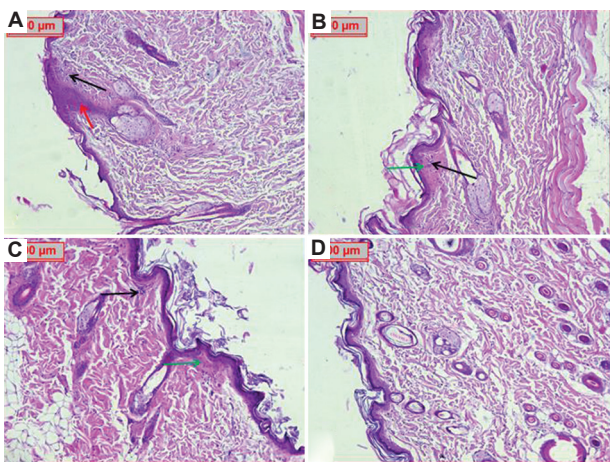

Figure 6. Hematoxylin and eosin staining showing histopathological changes in the skin of (A) negative control (Group 2), (B) blank formulation (Group 3), (C) free fluconazole (Group 4), and (D) F2 (Group 5). Scale bars: 200 μm; magnifications: ×100. Notes: Black arrow: Inflammation; Red arrow: Spongiosis formation; Green arrow: Keratinization.

inflammatory cell infiltration, marked keratinization, and hyperkeratosis (**Figure 6C**). On the other hand, treatment with our drug formulation (Group 5) markedly improved healing (**Figure 6D**). A normal skin structure was observed as a thin layer of keratin covering the completely regenerated epidermis. In addition, the dermal layer was normal without any inflammatory cells or edematous areas.

4. Conclusion

The present study demonstrates that FLU–LNP–CHI hydrogel promoted wound healing in a *C. albicans*-infected rat excision model. The enhanced healing response, supported by histopathological findings and *in vitro* antifungal activity, suggests that FLU–LNP–CHI may be a promising topical approach for managing fungus-infected wounds. However, further *in vivo* investigations incorporating quantitative fungal burden analysis and molecular markers of inflammation and tissue repair are warranted to fully elucidate its therapeutic potential, particularly in the context of antifungal resistance.

Acknowledgement
None.

Financial support
None.

Conflicts of interest statement
The authors have no financial or personal interests that could be perceived as influencing the content of this work.

Author contributions
Conceptualization: ESS; *Formal analysis*: MAW, SAI, AAH, MES, and AAS; *Investigation*: MAW, SAI, AAH, and MES; *Methodology*: MAW, SAI, AAH, and MES; *Visualization:* ESS; *Writing—original draft*: All authors; *Writing—review & editing*: RMK.

Ethical approval and consent to participate
This research was conducted in accordance with the National Institutes of Health's guidelines for the use and care of laboratory animals (NIH Publication No. 8023, revised 1978) and the Animal Research Reporting of *In Vivo* Experiments (ARRIVE) methodology Furthermore, this investigation was approved by the Medical Research Ethics Committee of the National Research Center in Giza, Egypt (approval number 0980223).

Consent for publication
Not applicable.

Availability of data
Data are available from the corresponding author on request.

References

1. Kaiser P, Wächter J, Windbergs M. Therapy of infected wounds: Overcoming clinical challenges by advanced drug delivery systems. *Drug Deliv Transl Res.* 2021;11:1545-1567. doi: 10.1007/s13346-021-00932-7
2. Nejati H, Farahpour MR, Nagadehi MN. Topical rosemary officinalis essential oil improves wound healing against disseminated *Candida albicans* infection in rat model. *Comp Clin Pathol.* 2015;24:1377-1383. doi: 10.1007/s00580-015-2086-z
3. Bachhav YG, Patravale VB. Microemulsion based vaginal gel of

fluconazole: Formulation, *in vitro* and *in vivo* evaluation. *Int J Pharm.* 2009;365(1-2):175-179.
doi: 10.1016/j.ijpharm.2008.08.021

4. Rençber S, Karavana SY, Yilmaz FF, *et al.* Formulation and evaluation of fluconazole loaded oral strips for local treatment of oral candidiasis. *J Drug Deliv Sci Technol.* 2019;49:615-621.
doi: 10.1016/j.jddst.2018.12.035
5. Delshadi R, Bahrami A, McClements DJ, Moore MD, Williams L. Development of nanoparticle-delivery systems for antiviral agents: A review. *J Control Release.* 2021;331:30-44.
doi: 10.1016/j.jconrel.2021.01.017
6. Khan A, Aqil M, Imam SS, *et al.* Temozolomide loaded nano lipid based chitosan hydrogel for nose to brain delivery: Characterization, nasal absorption, histopathology and cell line study. *Int J Biol Macromol.* 2018;116:1260-1267.
doi: 10.1016/j.ijbiomac.2018.05.079
7. Hung YH, Chou WC. Chitosan for suspension performance and viscosity of MWCNTs. *Int J Chem Eng Applic.* 2012;3(5):347.
doi: 10.7763/IJCEA.2012.V3.215
8. Tan Q, Liu W, Guo C, Zhai G. Preparation and evaluation of quercetin-loaded lecithin-chitosan nanoparticles for topical delivery. *Int J Nanomedicine.* 2011;6:1621-1630.
doi: 10.2147/IJN.S22411
9. Mohamed FH, El-sissi AF, Ismail SA, Ismail SA, Hashem AM. The potentiality of using chitosan and its enzymatic depolymerized derivative chito-oligosaccharides as immunomodulators. *J Appl Pharm Sci.* 2018;8(12):132-139.
doi: 10.7324/JAPS.2018.81215
10. Atay O, Selçk F. Quantitative determination of fluconazole by infrared spectrophotometry. *Anal Lett.* 1996;29(12):2163-2176.
doi: 10.1080/00032719608002239
11. Khan MM, Madni A, Tahir N, *et al.* Co-delivery of curcumin and cisplatin to enhance cytotoxicity of cisplatin using lipid-chitosan hybrid nanoparticles. *Int J Nanomedicine.* 2020;15:2207-2217.
doi: 10.2147/ijn.S247893
12. Shalaby ES, Abdelhameed MF, Ismail SA, Ahmed YH, Aboutaleb S. Innovative Indian propolis loaded carnauba wax based lipid structured nanocarriers: Preparation, characterization and *in vitro/in vivo* antifungal activities. *BioNanoScience.* 2024:14(2):1726-1743.
doi: 10.1007/s12668-024-01361-9
13. Shalaby ES, Aboutaleb S, Ismail SA, Yassen NN, Sedik AA. Chitosan tamarind-based nanoparticles as a promising approach for topical application of curcumin intended for burn healing: *In vitro* and *in vivo* study. *J Drug Target.* 2023;31(10):1081-1097.
doi: 10.1080/1061186X.2023.2276662
14. Khalid A, Ahmed N, Qindeel M, Asad MI, Khan GM, Ur Rehman A. Development of novel biopolymer-based nanoparticles loaded cream for potential treatment of topical fungal infections. *Drug Dev Ind Pharm.* 2021;47(7):1090-1099.
doi: 10.1080/03639045.2021.1957914
15. Abo-Elseoud WS, Hassan ML, Sabaa MW, Basha M, Hassan EA, Fadel SM. Chitosan nanoparticles/cellulose nanocrystals nanocomposites as a carrier system for the controlled release of repaglinide. *Int J Biol Macromol.* 2018;111:604-613.
doi: 10.1016/j.ijbiomac.2018.01.044
16. Khalil RM, Abdelhameed MF, Abou Taleb S, El-Saied MA, Shalaby ES. Preparation and characterisation of esculetin-loaded nanostructured lipid carriers gels for topical treatment of UV-induced psoriasis. *Pharm Dev Technol.* 2024;29(8):886-898.
doi: 10.1080/10837450.2024.2407854
17. Khalil RM, El Arini SK, AbouSamra MM, Zaki HS, El-Gazaerly ON, Elbary AA. Development of lecithin/chitosan nanoparticles for promoting topical delivery of propranolol hydrochloride: Design, optimization and *in-vivo* evaluation. *J Pharm Sci.* 2021;110(3):1337-1348.
doi: 10.1016/j.xphs.2020.11.025
18. Ammar HO, Ghorab MM, Mostafa DM, *et al.* Development of folic acid-loaded nanostructured lipid carriers for topical delivery: Preparation, characterisation and *ex vivo* investigation. *J Microencapsul.* 2020;37(5):366-383.
doi: 10.1080/02652048.2020.1761904
19. Pipe CJ, Majmudar TS, McKinley GH. High shear rate viscometry. *Rheol Acta.* 2008;47:621-642.
doi: 10.1007/s00397-008-0268-1
20. Beaulac C, Clement-Major S, Hawari J, Lagace J. *In vitro* kinetics of drug release and pulmonary retention of microencapsulated antibiotic in liposomal formulations in relation to the lipid composition. *J Microencapsul.* 1997;14(3):335-348.
doi: 10.3109/02652049709051137
21. Shamma RN, Sayed S, Sabry NA, El-Samanoudy SI. Enhanced skin targeting of retinoic acid spanlastics: *In vitro* characterization and clinical evaluation in acne patients. *J Liposome Res.* 2019;29(3):283-290.
doi: 10.1080/08982104.2018.1552706
22. Gong C, Lu C, Li B, Shan M, Wu G. Injectable dopamine-modified poly (α,β-aspartic acid) nanocomposite hydrogel as bioadhesive drug delivery system. *J Biomed Mater Res Part A.* 2017;105(4):1000-1008.
doi: 10.1002/jbm.a.35931
23. Balouiri M, Sadiki M, Ibnsouda SK. Methods for *in vitro* evaluating antimicrobial activity: A review. *J Pharm Anal.* 2016;6(2):71-79.
doi: 10.1016/j.jpha.2015.11.005
24. Brand-Williams W, Cuvelier ME, Berset C. Use of a free radical method to evaluate antioxidant activity. *LWT Food Sci Technol.* 1995;28(1):25-30.
doi: 10.1016/S0023-6438(95)80008-5
25. Sasidharan S, Nilawatyi R, Xavier R, Latha LY, Amala R. Wound healing potential of *Elaeis guineensis* jacq leaves in an infected albino rat model. *Molecules.* 2010;15(5):3186-3199.
doi: 10.3390/molecules15053186
26. Otto F, Van Hoogevest P, Syrowatka F, Heinl V, Neubert RH. Assessment of the applicability of HLB values for natural phospholipid emulsifiers for preparation of stable emulsions. *Pharmazie.* 2020;75(8):365-370.
doi: 10.1691/ph.2020.9174
27. Estiasih T, Marianty R, Ahmadi K. Characteristics and emulsifying properties of structured phospholipids from palm pressed fiber and omega-3 fatty acid concentrates from by-products of fish processing by enzymatic acidolysis. *J Food Sci Technol.* 2021;58(10):3689-3700.
doi: 10.1007/s13197-020-04827-2
28. Kunieda H, Ohyama KI. Three-phase behavior and HLB numbers of bile salts and lecithin in a water-oil system. *J Colloid Interf Sci.* 1990;136(2):432-439.
doi: 10.1016/0021-9797(90)90390-A
29. Bnyan R, Khan I, Ehtezazi T, *et al.* Surfactant effects on lipid-based vesicles properties. *J Pharm Sci.* 2018;107(5):1237-1246.
doi: 10.1016/j.xphs.2018.01.005
30. El-Nesr OH, Yahiya SA, El-Gazayerly ON. Effect of formulation design and freeze-drying on properties of fluconazole multilamellar liposomes. *Saudi Pharm J.* 2010;18(4):217-224.
doi: 10.1016/j.jsps.2010.07.003
31. El-Ridy MS, Abdelbary A, Essam T, Abd El-Salam RM, Aly Kassem AA. Niosomes as a potential drug delivery system for increasing the efficacy and safety of nystatin. *Drug Dev Ind Pharm.* 2011;37(12):1491-1508.
doi: 10.3109/03639045.2011.587431
32. Pople PV, Singh KK. Development and evaluation of topical formulation containing solid lipid nanoparticles of vitamin A. *AAPS PharmSciTech.* 2006;7:E63-E69.
doi: 10.1208/pt070491
33. Fan Y, Yen CW, Lin HC, *et al.* Automated high-throughput preparation and characterization of oligonucleotide-loaded lipid nanoparticles. *Int J Pharm.* 2021;599:120392.
doi: 10.1016/j.ijpharm.2021.120392
34. Priyanka K, Sathali AA. Preparation and evaluation of montelukast sodium loaded solid lipid nanoparticles. *J Young Pharm.* 2012;4(3):129-137.
doi: 10.4103/0975-1483.100016
35. Weiss J, Decker EA, McClements DJ, Kristbergsson K, Helgason T, Awad T. Solid lipid nanoparticles as delivery systems for bioactive food components. *Food Biophysics.* 2008;3(2):146-154.
doi: 10.1007/s11483-008-9065-8
36. He Q, Gong K, Ao Q, *et al.* Positive charge of chitosan retards blood coagulation on chitosan films. *J Biomater Appl.* 2013;27(8):1032-1045.
doi: 10.1177/0885328211432487
37. Dong W, Ye J, Wang W, *et al.* Self-assembled lecithin/chitosan nanoparticles based on phospholipid complex: A feasible strategy to

improve entrapment efficiency and transdermal delivery of poorly lipophilic drug. *Int J Nanomedicine*. 2020;15:5629-5643.
doi: 10.2147/ijn.S261162
38. Şenyiğit T, Sonvico F, Barbieri S, Özer Ö, Santi P, Colombo P. Lecithin/chitosan nanoparticles of clobetasol-17-propionate capable of accumulation in pig skin. *J Control Release*. 2010;142(3):368-373.
doi: 10.1016/j.jconrel.2009.11.013
39. Onugwu AL, Attama AA, Nnamani PO, Onugwu SO, Onuigbo EB, Khutoryanskiy VV. Development and optimization of solid lipid nanoparticles coated with chitosan and poly(2-ethyl-2-oxazoline) for ocular drug delivery of ciprofloxacin. *J Drug Deliv Sci Technol*. 2022;74:103527.
doi: 10.1016/j.jddst.2022.103527
40. Anwer MK, Iqbal M, Muharram MM, *et al*. Development of lipomer nanoparticles for the enhancement of drug release, anti-microbial activity and bioavailability of delafloxacin. *Pharmaceutics*. 2020;12(3):252.
doi: 10.3390/pharmaceutics12030252
41. Haidar ZS, Hamdy RC, Tabrizian M. Protein release kinetics for core-shell hybrid nanoparticles based on the layer-by-layer assembly of alginate and chitosan on liposomes. *Biomaterials*. 2008;29(9):1207-1215.
doi: 10.1016/j.biomaterials.2007.11.012
42. Alkhalidi HM, Hosny KM, Rizg WY. Oral gel loaded by fluconazole-sesame oil nanotransfersomes: Development, optimization, and assessment of antifungal activity. *Pharmaceutics*. 2021;13(1):27.
doi: 10.3390/pharmaceutics13010027
43. Wu PS, Li YS, Kuo YC, Tsai SJJ, Lin CC. Preparation and evaluation of novel transfersomes combined with the natural antioxidant resveratrol. *Molecules*. 2019;24(3):600.
doi: 10.3390/molecules24030600
44. Wang T, Luo Y. Chitosan hydrogel beads functionalized with thymol-loaded solid lipid-polymer hybrid nanoparticles. *Int J Mol Sci*. 2018;19(10):3112.
doi: 10.3390/ijms19103112
45. Tahir N, Madni A, Balasubramanian V, *et al*. Development and optimization of methotrexate-loaded lipid-polymer hybrid nanoparticles for controlled drug delivery applications. *Int J Pharm*. 2017;533(1):156-168.
doi: 10.1016/j.ijpharm.2017.09.061
46. Westesen K, Siekmann B. Investigation of the gel formation of phospholipid-stabilized solid lipid nanoparticles. *Int J Pharm*. 1997;151(1):35-45.
doi: 10.1016/S0378-5173(97)04890-4
47. Fang B, Watanabe H, Isobe K, Handa A, Nakagawa K. The manufacturing of lactobacillus microcapsules by freezing with egg yolk: The analysis of microstructure and the preservation effect against freezing and acid treatments. *J Agric Food Res*. 2021;6:100221.
doi: 10.1016/j.jafr.2021.100221
48. Sadeghi AM, Dorkoosh FA, Avadi MR, *et al*. Permeation enhancer effect of chitosan and chitosan derivatives: Comparison of formulations as soluble polymers and nanoparticulate systems on insulin absorption in Caco-2 cells. *Eur J Pharm Biopharm*. 2008;70(1):270-278.
doi: 10.1016/j.ejpb.2008.03.004
49. Mahjour M, Mauser B, Rashidbaigi Z, Fawzi MB. Effect of egg yolk lecithins and commercial Soybean lecithins on *in vitro* skin permeation of drugs. *J Control Release*. 1990;14(3):243-252.
doi: 10.1016/0168-3659(90)90164-O
50. Abd El Azim H, Nafee N, Ramadan A, Khalafallah NM. Liposomal buccal mucoadhesive film for improved delivery and permeation of water-soluble vitamins. *Int J Pharm*. 2015;488(1-2):78-85.
doi: 10.1016/j.ijpharm.2015.04.052
51. Ing LY, Zin NM, Sarwar A, Katas H. Antifungal activity of chitosan nanoparticles and correlation with their physical properties. *Int J Biomater*. 2012;2012(1):632698.
doi: 10.1155/2012/632698
52. El Rabey HA, Almutairi FM, Alalawy AI, *et al*. Augmented control of drug-resistant *Candida* spp. Via fluconazole loading into fungal chitosan nanoparticles. *Int J Biol Macromol*. 2019;141:511-516.
doi: 10.1016/j.ijbiomac.2019.09.036
53. Comino-Sanz IM, López-Franco MD, Castro B, Pancorbo-Hidalgo PL. The role of antioxidants on wound healing: A review of the current evidence. *J Clin Med*. 2021;10(16):3558.
doi: 10.3390/jcm10163558
54. Nasab ME, Takzaree N, Saffari PM, Partoazar A. *In vitro* antioxidant activity and *in vivo* wound-healing effect of lecithin liposomes: A comparative study. *J Comp Effect Res*. 2019;8(8):633-643.
doi: 10.2217/cer-2018-0128
55. Ismail SA, El-Sayed HS, Fayed B. Production of prebiotic chitooligosaccharide and its nano/microencapsulation for the production of functional yoghurt. *Carbohydr Polym*. 2020;234:115941.
doi: 10.1016/j.carbpol.2020.115941
56. Mei L, Ji Q, Jin Z, *et al*. Nano-microencapsulation of tea seed oil via modified complex coacervation with propolis and phosphatidylcholine for improving antioxidant activity. *Lwt*. 2022;163:113550.
doi: 10.1016/j.lwt.2022.113550

Received: May 9, 2025
Revised: December 30, 2025
Accepted: January 7, 2026
Available online: July 16, 2026